Predicting the Fraction of Mixing Between Latex Particles

Remi Casier, Mario Gauthier, Jean Duhamel

Institute for Polymer Research, Waterloo Institute for Nanotechnology, Department of Chemistry, University of Waterloo, 200 University Ave. W., Waterloo, ON, Canada N2l 3G1

Introduction

Over the years, latex paints have found many industrial applications including their use to form films for decorative and protective purposes. The properties of a film formed from a latex dispersion are directly related to the extent of coalescence between adjacent particles.[1] For example, a film in which the particles are unable to coalesce will result in a mechanically weak and highly permeable film, whereas a highly coalesced film will be much more mechanically robust and provide superior protection against external elements. As such, the quantification of the fraction of mixing (f_m) between adjacent particles has been actively studied for over 30 years. There have been several techniques developed to quantitatively probe f_m, such as small angle neutron scattering (SANS),[2] fluorescence resonance energy transfer (FRET),[3] and most recently pyrene excimer fluorescence (PEF).[4] The introduction of PEF allowed for the determination of f_m in a simple manner by monitoring the change in the ratio of the steady-state fluorescence intensity of pyrene excimer (I_E) over that of the monomer (I_M), namely the I_E/I_M ratio, as a function of annealing time. In PEF measurements, a film is prepared by mixing a small amount of pyrene-labeled particles in a matrix of non-fluorescent particles. Initially, all pyrene labels are contained within the few pyrene-labeled particles, which results in a relatively high I_E/I_M ratio. As the film anneals, the pyrene-labeled polymer chains diffuse out of the initial particle boundaries into the surrounding unlabled matrix. As this occurs, the amount of intermolecular-excimer formed decreases, resulting in a drop in the I_E/I_M ratio with increasing annealing time. By monitoring the decrease in I_E/I_M over the course of annealing, f_m could be calculated as a function of annealing time.

Using the PEF method, the fraction of mixing in two different films were studied, one film prepared with pyrene-labeled polymers having a high M_w of 820 kg·mol^{-1}, and the other with a lower M_w of 360 kg·mol^{-1}. Plots of f_m versus annealing time were determined for each film at nine annealing temperatures ranging from 75 to 119 °C. The profiles were then compared to examine the effect of temperature and molecular weight on the rate of coalescence in the films. Analysis of the f_m profiles led to the implementation of a simple method that yields the annealing time required to reach a desired f_m value at a given temperature. In turn, this procedure provided the activation energy necessary for PBMA chains to diffuse across the latex particle boundary at the onset of annealing.

Experimental

Latex Preparation: The poly(*n*-butyl methacrylate) (PBMA) latex was prepared via a semi-batch emulsion polymerization process at 80 °C using dioctyl sodium sulfosuccinate (AOT) as a surfactant and ammonium persulfate (APS) as an initiator. The pyrene-labeled PBMA latex (Py-PBMA) was prepared in a similar manner, with the main difference being the addition of ca. 2 mol% of a pyrene-labeled monomer. The full details of the synthesis have been described elsewhere.[4]

Film Preparation: Two PBMA films were studied consisting of Py-PBMA with M_w of

Table 1: Composition of the films used to probe film formation and polymer diffusion.

Film	Latex	Pyrene Content (mol%)	Particle Size (nm)	PSD *	M_w (kg·mol^{-1})	$Đ$ **	Weight Fraction
1	Py-PBMA-Latex-1	1.9	119	0.02	820	1.9	0.05
	PBMA-Latex-1	0	96	0.01	1,000	2.0	0.95
2	Py-PBMA-Latex-2	1.8	123	0.01	360	1.8	0.05
	PBMA-Latex-2	0	120	0.02	320	1.7	0.95

*Particle size dispersity; **Molecular weight dispersity

820 and 360 kg·mol^{-1}for films 1 and 2, respectively. As can be seen in Table 1, the properties of the latexes used to prepare each film were similar. The latex dispersions were cast onto a quartz plate and allowed to dry under nitrogen overnight before they were annealed.

Film Annealing: The dried films were annealed in a glass tube submerged in a constant-temperature oil bath. The tube was sealed with a rubber septum to maintain a nitrogen atmosphere and equipped with a thermocouple probe to monitor the internal temperature. After annealing, the films were placed on an aluminum block in order to quickly cool the film to room temperature to prevent any further coalescence during the fluorescence measurements. After measuring the fluorescence of a film, the film was then placed back into the tube for further annealing.

Steady-State Fluorescence: Measurements were conducted using a Photon Technology International steady-state fluorometer equipped with a xenon arc lamp. The films were excited at 344 nm and the emission was scanned from 350 to 600 nm using a front-face geometry setup. The I_E/I_M ratio was calculated using the area from 392 to 398 nm for the monomer (I_M) and from 500 to 530 nm for the excimer (I_E).

Results and Discussion

For both films 1 and 2 outlined in Table 1, the steady-state fluorescence spectrum was monitored over time for a total of nine annealing temperatures ranging from 75 to 119 °C. Figure 1 displays the change in the steady-state fluorescence spectrum for film 1 at an annealing temperature of 102 °C. The film exhibited the highest amount of excimer before annealing, corresponding to

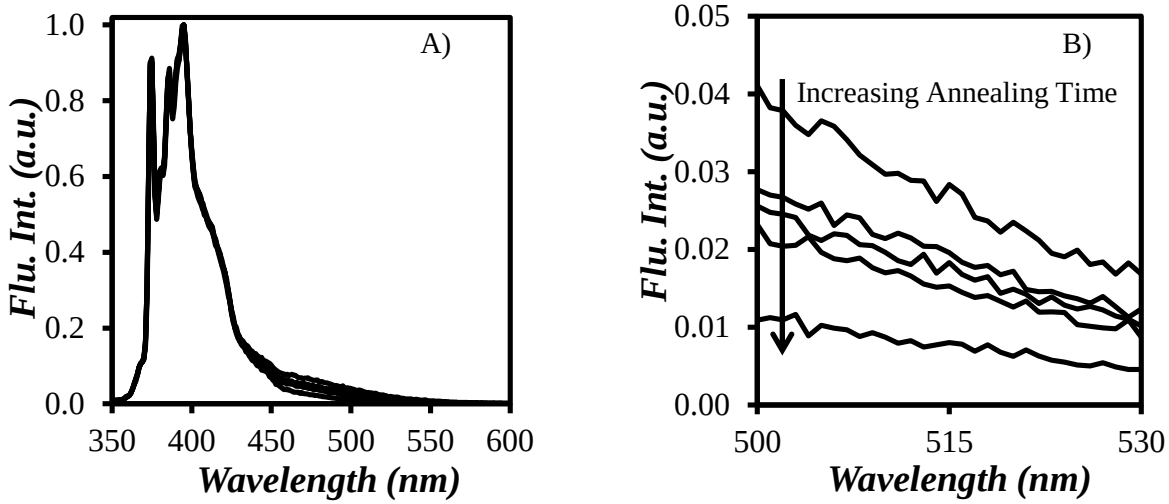

Figure 1: Steady-state fluorescence spectra obtained for film 1 (Table 1) at 102 °C A) over the entire region scanned and B) the expanded excimer region. Top to bottom: t_{an} = 0, 25, 110, 560 min., and a homogeneous film. λ_{ex} = 344 nm.

an I_E/I_M ratio of 0.13. As film formation occurred, and the polymer chains containing pyrene diffused into the surrounding particles, the fluorescence intensity of the excimer decreased, reaching a value of 0.04 for a fully annealed film. Similar changes in the fluorescence spectrum were observed for both films 1 and 2 over all temperature ranges. Using the I_E/I_M ratios, the fraction of mixing f_m between adjacent particles in a film at annealing time t_{an} was calculated using Equation 1, where t_∞ denotes a homogeneous film.

$$f_m(t_{an}) = \frac{\frac{I_E}{I_M}(t_{an}) - \frac{I_E}{I_M}(t_{an}=0)}{\frac{I_E}{I_M}(t_\infty) - \frac{I_E}{I_M}(t_{an}=0)} \qquad (1)$$

In a plot of f_m as a function of annealing time, a typical shape was observed characterized by a rapid increase in f_m at short annealing times and a more gradual increase at longer annealing time, as depicted in Figures 2A and B. This typical profile likely arises from two distinct reasons: the rather large dispersity ($Đ$) of the polymer present in the film, and the initial configurational strain of the polymers held inside the initial particle boundaries of the latex particles.[2-4] In latex samples with large $Đ$, the early times of diffusion are dominated by the shorter chains, resulting in a rapid increase in f_m. The short chains quickly reach equilibrium in the film, at which point the diffusion of the larger chains begins to dominate, resulting in a slower but continuous increase in f_m. In addition to the effect of $Đ$, all of the polymer chains are initially confined within distinct particle boundaries, with the chains closer to the particle surface having a restricted number of configurations since the particle boundary limits their configurational space. These confined chains are expected to diffuse more quickly at early times to reduce this configurational strain, resulting in a larger increases in f_m at early times. In addition to annealing time, a quick inspection of Figures 2A and B shows that f_m increases with increasing annealing temperature and decreasing polymer molecular weight.

When the fraction of mixing was plotted against $ln(t_{an})$ in Figures 2 C and D, a strikingly simple trend was observed. Both plots for films 1 and 2 resulted in a nearly linear increase in f_m vs. annealing time at all the annealing temperatures. For each annealing temperature, the fraction of mixing was fitted with Equation 2.

$$f_m(T, t_{an}) = A(T)\cdot\ln(t_{an}) + B(T) \qquad (2)$$

Equation 2 assumes a linear trend in the semi-log plot of f_m versus t_{an} as observed in Figures 2C and D, where the slope (A) and intercept (B) are dependent upon the annealing temperature and polymer structure. Next, A and B were plotted against temperature in Figure 3. The plots of A and B against temperature also yielded linear trends. The A values remained nearly constant at all annealing temperatures for film 2, and only increased slightly with temperature for film 1. This indicates that the slope of f_m versus $ln(t_{an})$ was similar for both films and independent of the annealing temperature. In contrast, the B values increased rapidly with the annealing temperature. The increase in B was higher for film 2, containing the lower molecular weight polymer. The linear trends for A and B were then fitted with a straight line. The linear trends were then used to construct equations for A and B as a function of the annealing temperature. These equations were then substituted back into Equation 2, resulting in Equations 3 and 4 for films 1 and 2, respectively.

$$f_m(T, t_{an}) = \left(6.71\times10^{-4}T - 0.184\right)\ln(t_{an}) + \left(7.74\times10^{-3}T - 2.65\right) \qquad (3)$$

$$f_m(T, t_{an}) = \left(-0.172\times10^{-4}T + 0.144\right)\ln(t_{an}) + \left(1.16\times10^{-2}T - 4.05\right) \qquad (4)$$

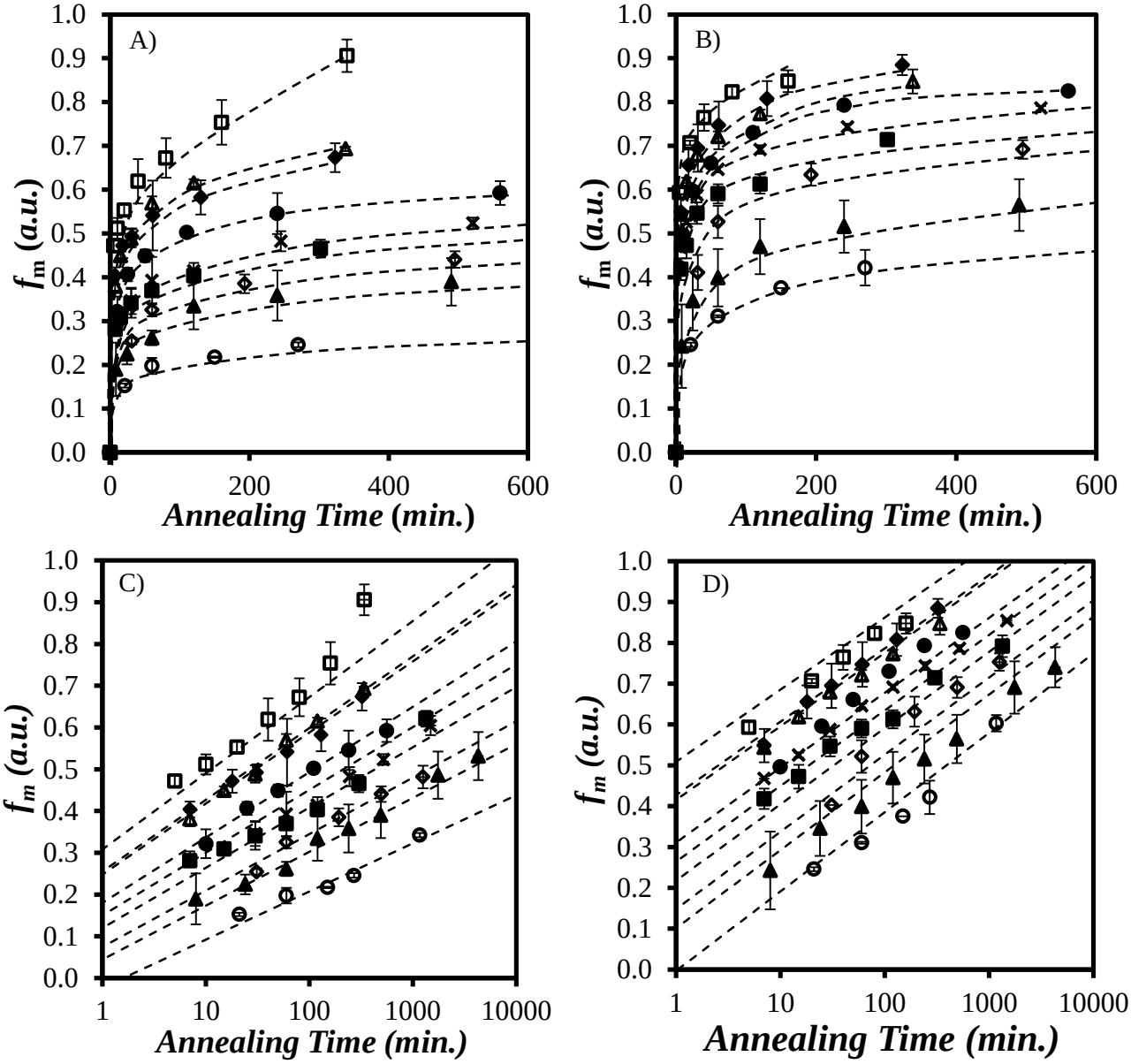

Figure 2: Fraction of mixing for A,C) film 1 (Py-PBMA M_w = 820 kg·mol^{-1}) and B,D) film 2 (Py-PBMA M_w = 360 kg·mol^{-1}) plotted with t_{an} on a A,B) linear and C,D) logarithmic axis. t_{an} = 119 (□), 112 (◆), 111 (△), 102 (●), 98 (×), 94 (■), 88 (◇), 84 (▲), and 75 (○) °C. The dashed lines A,B) were only added to guide the eyes, and C,D) display the predicted f_m values from Equations 3 and 4.

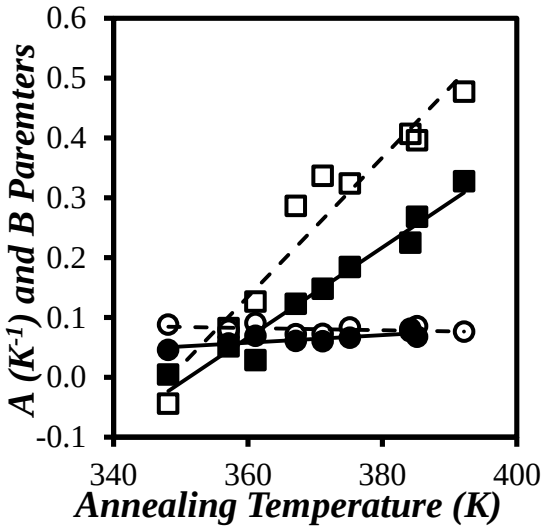

Figure 3: Plot of the slopes (A, circles) and intercepts (B, squares) determined from f_m vs. $ln(t_{an})$ lines for film 1 (solid) and film 2 (hollow).

To validate our method, the f_m values calculated from Equations 3 and 4 were compared with the experimental f_m values reported in Figures 2C and D. The predicted f_m values for film 1 agree closely with the experimental values, with nearly all of the experimental f_m values falling on the predicted trend. Similarly, the experimental f_m values obtained for film 2 lay close to the calculated values. However, some f_m values calculated for several annealing temperatures tended to deviate from the experimental values. Notably, the f_m values at an annealing temperature of 98 °C tended to be higher than the calculated values, while at 119 °C they tended to be lower. Despite these deviations, the majority of predicted trends displayed an overall good agreement with the experimental f_m values.

One interesting detail about Equations 3 and 4 is that they can be easily inverted to yield the annealing time as a function of temperature and fraction of mixing, as shown in Equations 5 and 6 for films 1 and 2, respectively. In effect, Equations 5 and 6 allow the experimentalist to predict how long a film should be annealed for to reach a given fraction of mixing, and ultimately predict the resulting properties of the film.

$$t_{an} = \exp\left(\frac{f_m(T,t_{an}) - (7.74\times10^{-3}T - 2.65)}{6.71\times10^{-4} - 0.184} \right) \quad (4)$$

$$t_{an} = \exp\left(\frac{f_m(T,t_{an}) - (1.16\times10^{-2}T - 4.05)}{-0.172\times10^{-4} + 0.144} \right) \quad (5)$$

One consequence of using a semi-log plot to predict f_m in Figures 2C and D is that the predicted tends for f_m will intercept the time axis at a value larger than zero. In other words, Equations 3 and 4 predict that there is a time delay before diffusion within the film can occur. This onset time $t_{an}(f_m=0)$ may be representative of the reptation time of the polymer chains confined in the original latex particles, which would take into account the reptation time of the unstrained chains and the additional strain of the chains due to the reduced number of configurations near the particle surface. Further inspection of Figures 2C and D shows that the onset time is typically larger for film 1, containing the higher molecular weight polymer, than film 2 for a given annealing temperature. Since larger chains reptate more slowly than shorter ones, it would be expected that the onset time would reflect the same trend and therefore the larger chains in film 1 should have a larger onset time. If we assume that the onset time of the polymer chains follows Arrhenius behaviour, a plot of $\ln(t_{an}(f_m=0))$ against the inverse of annealing temperature should be linear with the slope proportional to the energy barrier required for diffusion to begin. As seen in Figure 4, both films exhibit relatively straight lines with slopes corresponding to activation energies of 109 ± 13 and 169 ± 21 kJ·mol^{-1} for films 1 and 2, respectively. Interestingly, the activation energy is higher for film 2, containing the lower molecular weight polymer, than for film 1.

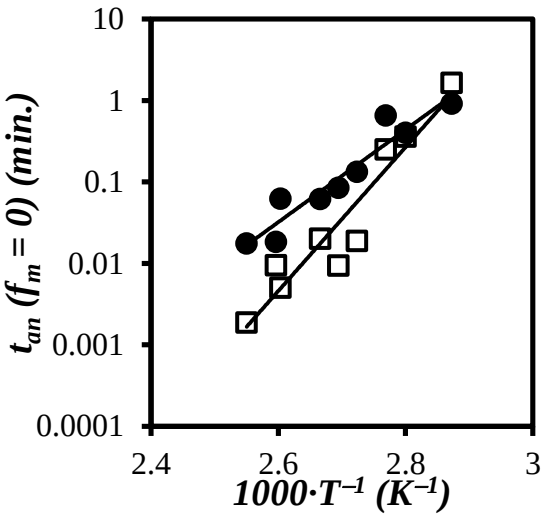

Figure 4: Arrhenius plot of the onset time predicted for film 1 (●) and film 2 (□) from the linear plot of f_m vs. $ln(t_{an})$.

Normally, the longer chains would be expected to have a larger activation energy. However, since the polymers are confined to latex particles when f_m=0, this result might reflect the difference in configurational strain of the polymers in films 1 and 2. Since the particle sizes are similar, the amount of configurational strain initially present will depend heavily on the polymer molecular weight, with larger chains having larger strain. The additional strain experienced by the larger chains results in a decrease of the activation energy required for the chains to diffuse across the latex boundaries.

In conclusion, a simple procedure was implemented to estimate the fraction of mixing between latex particles during film formation. A plot of f_m against $ln(t_{an})$ yielded a straight line at every annealing temperature, whose slope and intercept were employed to derive equations used to predict f_m. The predicted f_m values agreed quite closely with the experimental values for both films. As a first approximation, we believe that this method provides a simple tool that can be used to predict f_m. The equation can also simply be rearranged to estimate the annealing time or temperature required to reach a set f_m value. In future studies, the impact of additional parameters such as the particle size and polymer molecular weight could be investigated, in the hope of producing a universal equation for predicting f_m values. The t_{an} at which f_m reached zero in the plots of f_m vs. $ln(t_{an})$ were also determined. This so called onset time was then used to determine the activation energies of 109 ± 13 and 169 ± 21 kJ·mol^{-1} for the onset of diffusion for films 1 and 2, respectively. The lower E_a value of film 1 was attributed to the increased configurational strain present in the film 1 due to the larger polymer molecular weight.

References

1. Gauthier, C.; Guyot, A.; Perez, J.; Sindt, O. Film Formation and Mechanical Behavior of Polymer Laticies. *Film Formation in Waterborne Coatings*, American Chemical Society: Washington, DC **1996,** Chapter 10, pp 163–178.
2. Hahn, K.; Ley, G; Schuller, H.; Obethür, R. On Particle Coalescence in Latex Films. *Colloid Polym. Sci.* **1986**, *264*, 1092–1096.
3. Pekcan, Ö.; Winnik, M. A. Fluorescence Studies of Coalescence and Film Formation in Poly(methyl methacrylate) Nonaqueous Dispersion Particles. *Macromolecules* **1990**, *23*, 2673–2678.
4. Casier, R.; Gauthier, M.; Duhamel, J. Using Pyrene Excimer Fluorescence to Probe Polymer Diffusion in Latex Films. *Macromolecules* **2017**, *50*, 1635–1644.